Energy distribution and structure of gravitationally stratified coronal loops

K. Karampelas[1], T. Van Doorsselaere[1], M. Guo[1,2]

[1] Centre for mathematical Plasma Astrophysics, Department of Mathematics, KU Leuven

[2] Institute of space sciences, Shandong University, Weihai 264209, China

E-mail: kostas.karampelas@kuleuven.be

Aims of the current study

- Effects of gravity to energy dissipation
- Effects of driver strength
- Effects of resistivity and viscosity
- Spatial and temporal evolution of energy dissipation

Numerical models (from **Karampelas et al, in prep.**):

- 3D density enhanced, gravitationally stratified straight flux tube
- Loop Length: L=100 M
- Loop Radius: R=1 Mm
- Resolution: (δx,δy,δz)=(15.6, 15.6, 1526.5) km

Table: Physical parameters of our models. The index i (e) denotes the internal (external) values of (from) the tube.

Model	Period	Ti/Te	Ti (K)	Bz (G)	b	β	v0 (km/s)	Re	Rm
1	315	3	3e6	17.9	1000	0.097	2	1e8	1e8
2	287	3	3e6	17.9	1000	0.097	2 & 4	1e8	1e8
3	172	1/3	9e5	22.8	20	0.019	4	1e8	1e8
4	172	1/3	9e5	22.8	20	0.019	4	1e8	1e4
5	172	1/3	9e5	22.8	20	0.019	4	1e4	1e8

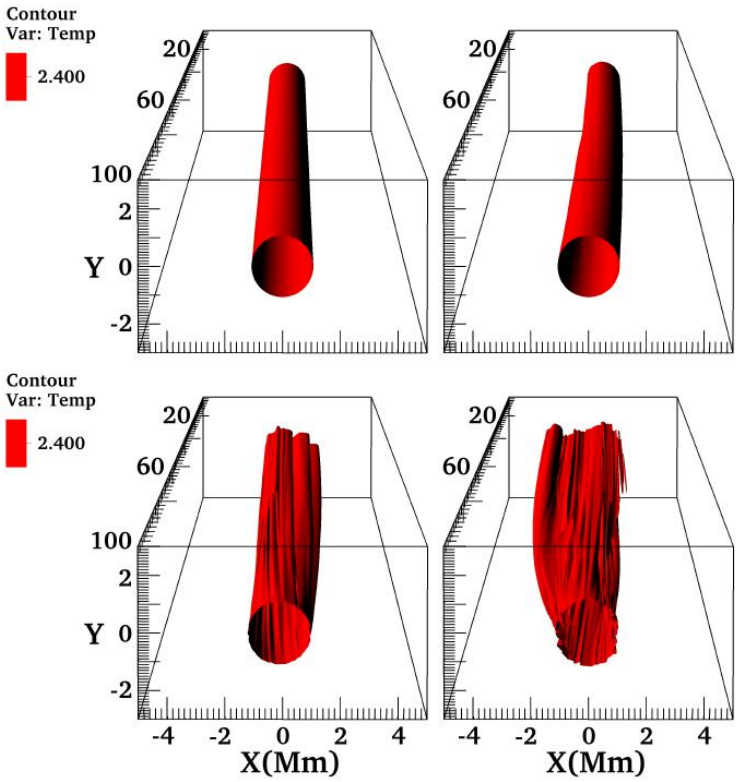

Movie 1 (eposter version): Temperature contour of a cold, gravitationally stratified flux tube, for a driver with v_0 =4 km/s, with period $P = 172$ s (model **3**). (Movie replaced by snapshots for $t = 0, 2.5P, 4.75P$ and $10P$).

Dynamical evolution of our models

1. Standing kink oscillation (movies. 1, 2 and 3), similar to the non-stratified case (see **Karampelas et al. 2017**).
2. Development of spatially extended **TWIKH** rolls for high values of resistivity and viscosity (Fig 1), with the use of a continuous driver.
3. Complete deformation of initial monolithic loop profile into a turbulent loop profile due to the developed TWIKH rolls.
4. Extensive mixing of plasma between the loop and the surrounding corona (see also poster by Van Doorsselaere T. for the DEM analysis).

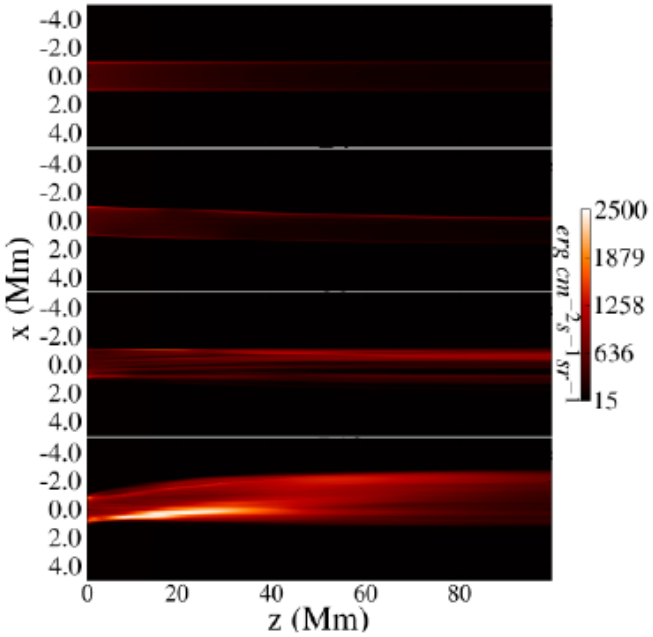

Movie 2 (eposter version): Integrated emission intensity of a cold, gravitationally stratified flux tube, for a driver with $v_0 = 4$ km/s, with period $P = 172$ s (model **3**). (Movie replaced by snapshots for $t = 0, 2.5P, 4.75P \; and \; 10P$).

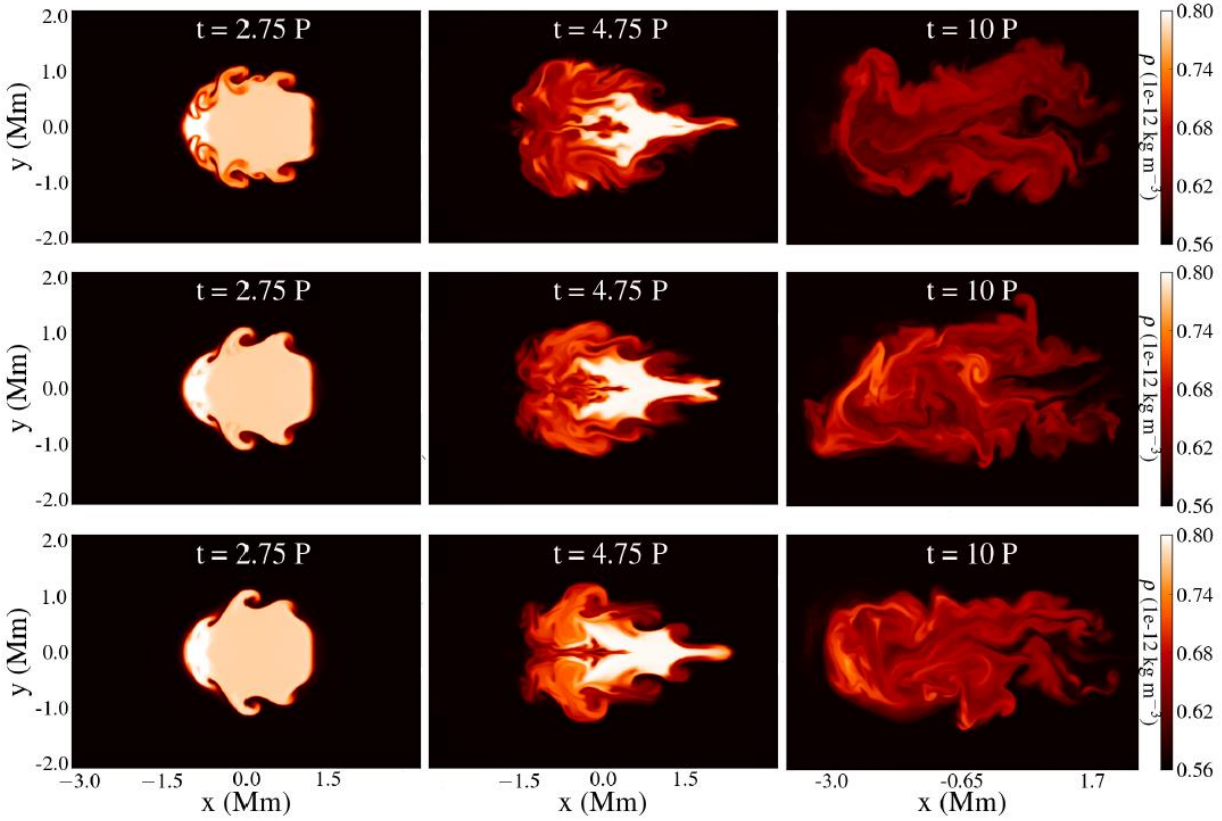

Figure 1: Loop cross-section at the apex for ideal (top), resistive (middle) and viscous (bottom) MHD. $P = 172$ s. Note the development of spatial expanded TWIKH rolls for all three cases.

Temperature profiles and wave heating

1. Energy dissipation gets stronger once the kinetic energy saturates (Fig. 2). Wave heating is stronger the more turbulent the loop cross-section becomes (also watch the talk by Guo M.).
2. Slight increase of gravitational energy, due to slight transfer of mass from the footpoint.
3. Energy power spectra (Fig.3) at the apex reveal a turbulent cross-section. The very steep slope (-2.8) hints towards a non-fully developed, non isotropic, compressible turbulence.
4. Resistivity and viscosity seem to lead to a slightly faster energy dissipation. Small deviations from the ideal case, due to the strong numerical dissipation.

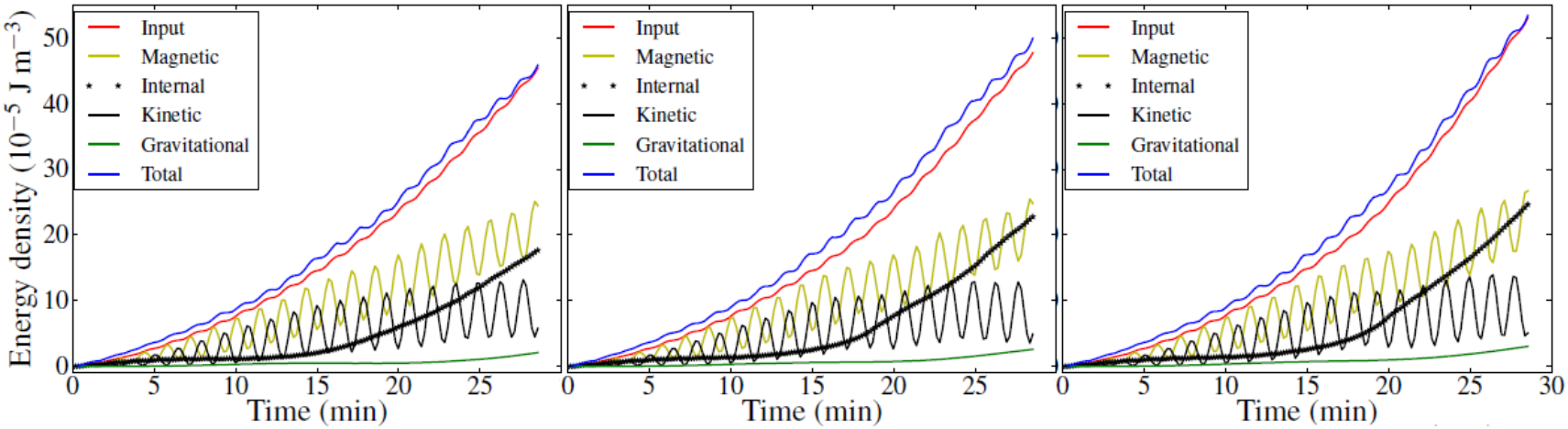

Figure 2: Input energy from the driver, internal and magnetic energy densities minus the fluxes from the open side boundaries, as well as the kinetic gravitational and total energy densities for models (3-idea, leftl) (4-resistive, middle) and (5-viscous, right).

Temperature profiles and wave heating

1. Energy dissipation gets stronger once the kinetic energy saturates (Fig. 1). Wave heating is stronger the more turbulent the loop cross-section becomes (also watch the talk by Guo M.).
2. Slight increase of gravitational energy, due to slight transfer of mass from the footpoint.
3. Energy power spectra (Fig.3) at the apex reveal a turbulent cross-section. The very steep slope (-2.8) hints towards a non-fully developed, non isotropic, compressible turbulence.
4. Resistivity and viscosity seem to lead to a slightly faster energy dissipation. Small deviations from the ideal case, due to the strong numerical dissipation.

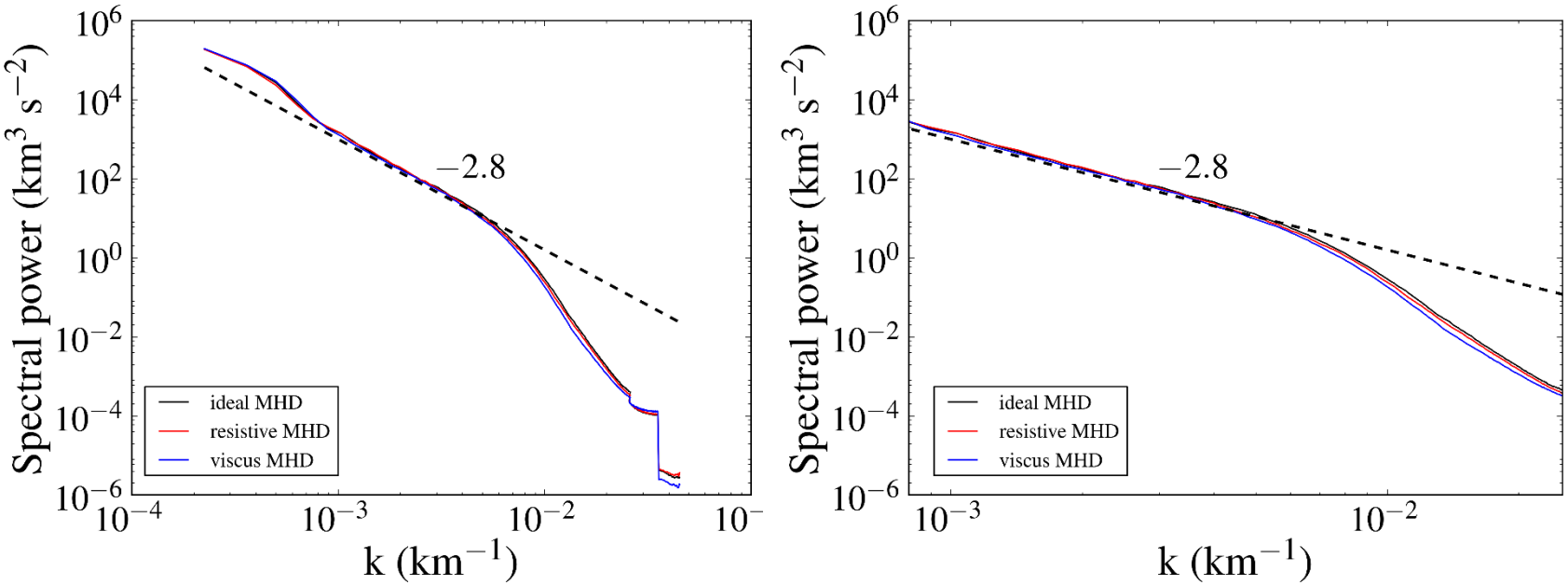

Figure 3: Energy spectra at the apex, for our model of a cold loop in ideal, resistive and viscous MHD. The signal is time averaged over the last 4 periods of the simulation (where the kinetic energy saturates), between 1032 1720s.

Temperature profiles and wave heating

5. Temperature peaks **~2e5 - 5e5 K** for models (1) and (2), at the apex, are attributed partially to adiabatic heating and partially to energy dissipation.
6. Average temperature increase: **~ 1e5 K** for models (1) and (2) inside the tube, near the apex and **~ 1e4 K** for models (3), (4) and (5) over the whole cross-section, near the apex and footpoint.

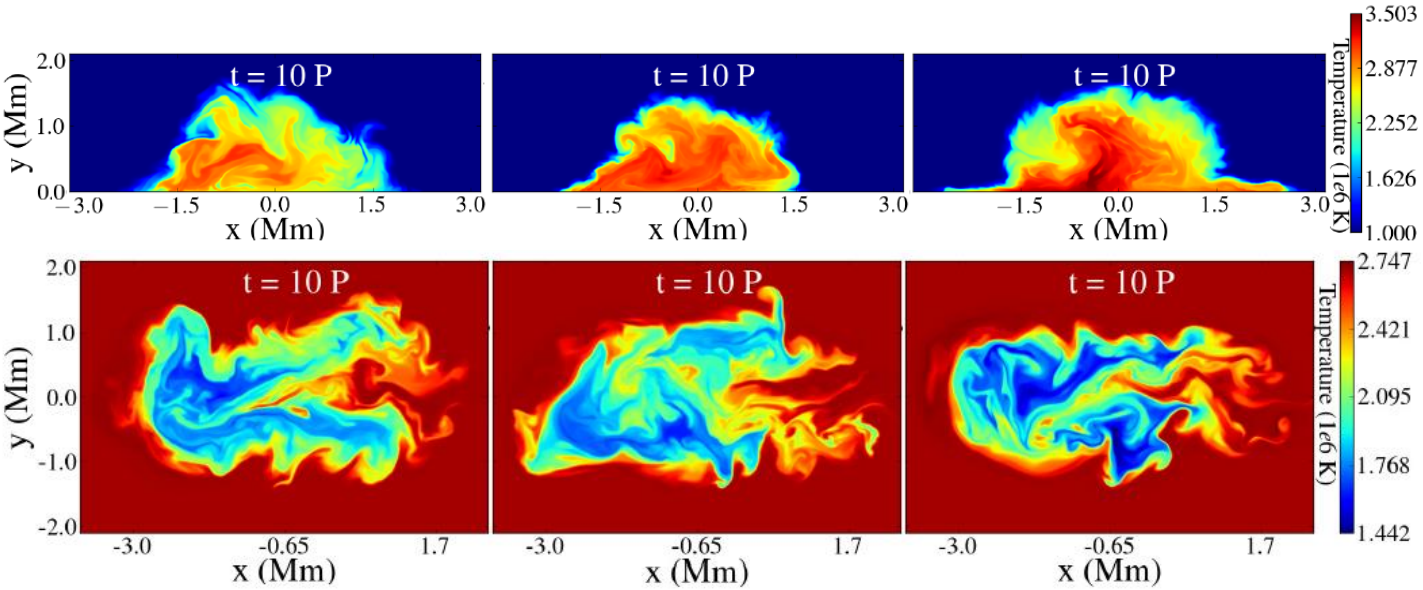

Figure 4: Temperature contours at the apex for models (1) and (2) for 2 km/s driver amplitude, and for model (2) with 4 km/s driver amplitude (top row). $P = 315$ and $P = 287$ s. Same, for models (3,) (4) and (5) (bottom row), with $P = 172$ s.

Temperature profiles and wave heating

6. Average temperature increase: **~ 1e5 K** for models (1) and (2) inside the tube, near the apex and **~ 1e4 K** for models (3), (4) and (5) over the whole cross-section, near the apex and footpoint.
7. Gravity reinforces the effects of wave heating (Fig. 5 and 6). The average temperature increase at the apex for model (2).
8. Stronger drivers lead to stronger heating (Fig. 6).
9. Models (3), (4) and (5): heating off the whole x-y plane at the apex and footpoint, despite the mixing with the colder loop plasma (Fig. 5).
10. Models (3), (4) and (5): Energy dissipation all along the loop axis.
11. Resistivity acts like a turbulent viscosity. Alternatively, shear viscosity seems to act like a form of effective resistivity. Similar spatial and temporal energy evolution.

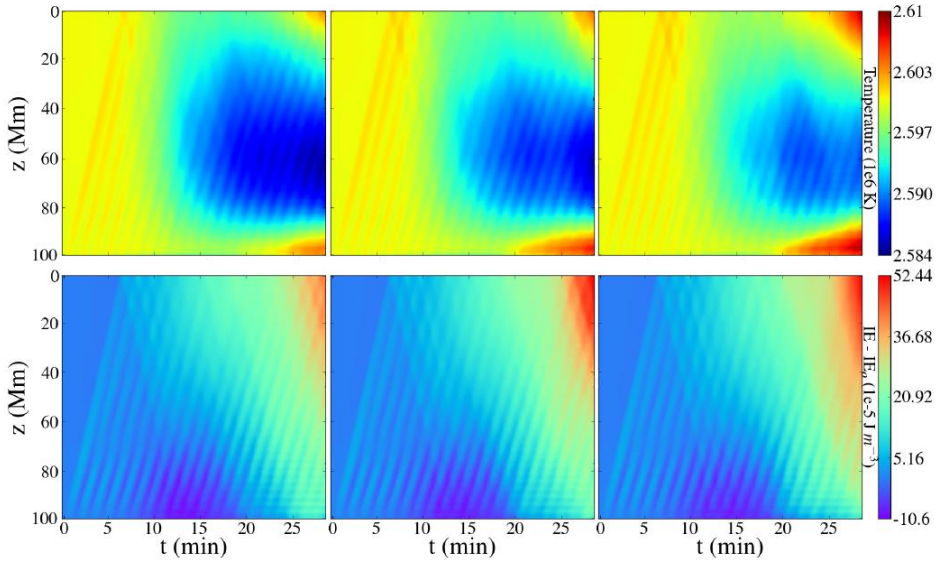

Figure 5: Average temperature (over the whole x-y plane) per height and over time (middle row) and average internal energy density temperature (over the whole x-y plane) (bottom row). From left to right:, model (3), (4) and (5).

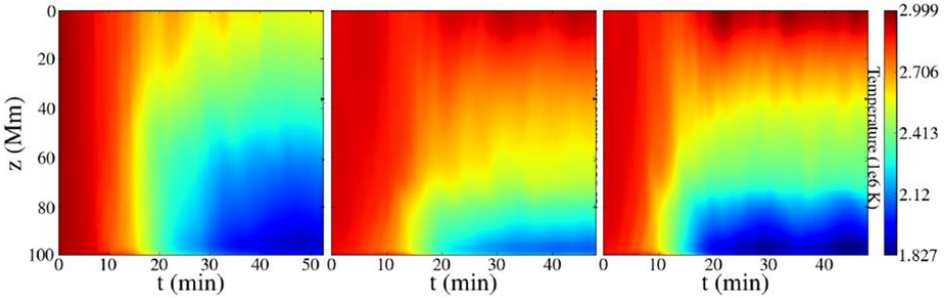

Figure 6: Average temperature inside the loop, per height and over time (bottom row). From left to right:, model (1), model (2) for 2 km/s driver amplitude and model (2) for 4 km/s driver amplitude.